Binding of a mobile hole by an impurity potential in the *t-J* model: Parity breaking

O. P. Sushkov and J. Oitmaa
School of Physics, University of New South Wales, Sydney 2052, Australia

(Received 27 August 2009; revised manuscript received 15 October 2009; published 24 November 2009)

We revisit the problem of a single hole moving in the background of the two-dimensional Heisenberg antiferromagnet. The hole is loosely bound by an impurity potential. We show that the bound state is generically a parity doublet: there are parametrically close bound states of opposite parity. Due to the degeneracy the bound state readily breaks local symmetries of the square lattice and this leads to formation of the long-range spiral distortion of the antiferromagnetic background. A direct analogy with van der Waals forces in atomic physics is discussed.

DOI: 10.1103/PhysRevB.80.195114 PACS number(s): 74.72.−h, 75.25.+z, 75.30.Fv

I. INTRODUCTION

The problem of single hole binding by an attractive potential in the *t-J* model is of fundamental importance. In the physics of doped Mott insulatoris and in particular in the physics of the cuprate superconductors, the system play a role analogous to the that played by the hydrogen atom in atomic physics.

We have in mind, for example, La_2CuO_4 with a La ion replaced by Sr. Alternatively it may be $Ca_2CuO_2Cl_2$ with a Ca ion replaced by Na. An important point is that the attractive center (Sr ion in La_2CuO_4 or Na ion in $Ca_2CuO_2Cl_2$) sits in the center of a square of four Cu sites. This means that the attractive potential itself does not break the local square lattice symmetry. There are various aspects of the bound state problem: the symmetry/parity of the bound state, the structure of the spin fabric, and in the end the particular value of the binding energy. We argue that the symmetry issues are the most important ones.

There have been several studies of the bound state problem. These are mainly small cluster exact diagonalizations.[1–4] A generic limitation of this approach is the small cluster size and as a consequence sensitivity to boundary conditions. In spite of this limitation a very important observation has been made already in the early work:[2] the ground state is almost degenerate with another state that has opposite parity. Dependent on the parameters of the model, the ground state belongs either to the two-dimensional E representation of the C_{4v} symmetry group of the Hamiltonian or to the A_1 representation.[4] However, there is always a very low-lying excitation of opposite parity.

A semiclassical solution of the bound state problem was obtained in Ref. 5. Generally a semiclassical approach can be justified in the limit of a large radius of the bound state. According to the semiclassical solution the bound state generates a long-range ($\propto 1/r$) spiral distortion of the spin fabric as it is shown in Fig. 1. The figure shows staggered spins. It is obvious from Fig. 1 that the semiclassical solution does not have a definite parity. It does not fit in any representation of the symmetry group of the square lattice. So the solution spontaneously breaks the local square lattice symmetry. On the other hand it is impossible to have a spontaneous violation of an exact symmetry of the Hamiltonian in a finite system. Therefore, the exact parameter that justifies the semiclassical solution[5] has remained unclear. The purpose of the present work is to elucidate this parameter and hence to elucidate the physical meaning of the solution with violation of exact symmetries. We show that the physics of this system is similar to the physics of a hydrogen atom in an external electric field. The parameter that justifies the semiclassical solution is the small splitting between states of opposite parity. The splitting scales as the binding-energy squared and hence it is infinitesimally small for a shallow bound state.

In the present paper we consider a local spin spiral produced by a single hole bound by an impurity potential. This problem represents a "hydrogen atom" of physics of cuprates. The spin spiral is not always related to impurities, the spin spiral of slightly different structure is developed at uniform doping as well. Formation of spin spirals is a generic property of the two-dimensional (2D) extended *t-J* model at small doping. A specific way of evolution from Mott insulator to finite doping as well as specific structure of the spin spiral depends on details such as presence/absence of impurities, presence/absence of the double layer splitting, etc. An overview of possible ways of evolution as well as comparison with experimental data is presented in Ref. 6.

The structure of the present paper is as follows. In Sec. II we explain the analogy with the hydrogen atom. In particular, we consider the conditions when a long-range tail of the dipole electric field can be generated by the atom. In Sec. III we briefly review known properties of an unbound single hole moving in the antiferromagnetic background of the *t-J* model. Section IV addresses the limiting case of very strong binding. Here we present results of exact diagonalizations for the 4×4 cluster embedded in an antiferromagnetic background. In Secs. V and VI we consider the weak binding limit and discuss symmetry properties of the bound states. Sec. VII addresses the parity breaking and generation of the local spin spiral. In Sec. VIII we exclude a possibility of the local charge density wave (CDW) formation. Our conclusions are presented in Sec. IX.

II. HYDROGEN ATOM

Consider a hydrogen atom in the ground $1s$ state. The size is about one Bohr radius, a_B. Since the atom is neutral the electric field at distances $r \gg a_B$ decays exponentially. Let us consider the same atom in the $n=2$ state, either the positive

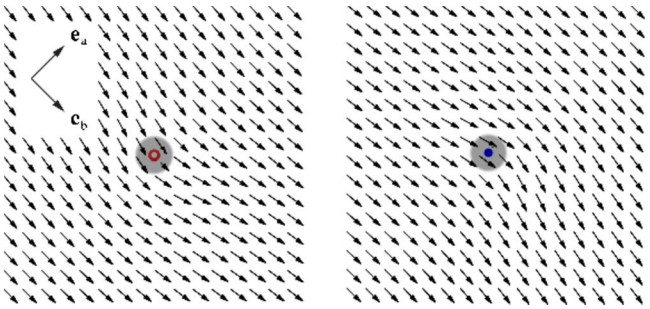

FIG. 1. (Color online). Distortion of the staggered spin fabric (small arrows) by the Sr-hole bound state. The left picture corresponds to the pseudospin directed out of the page and the right picture corresponds to the pseudospin directed in the page. Shaded area corresponds to the hole localization region. At large distances spins are directed along the orthorhombic *b* axis due to pinning by Dzyaloshinksi-Moriya and *XY* anisotropies.

parity $2s$ state or negative parity $2p$ state. Importantly, they are degenerate. Because of the degeneracy an infinitesimally small *external* electric field, $E_{ext} \to 0$, will mix the opposite parity states

$$\psi = \frac{1}{\sqrt{2}}|2s\rangle + \frac{1}{\sqrt{2}}|2p_0\rangle. \tag{1}$$

Here $|2p_0\rangle$ is the state with zero projection of the angular momentum in the direction of the external electric field. The state (1) possesses a static electric dipole moment $d \sim ea_B$. Hence, a static dipole electric potential and a static electric field are induced outside the atom, $r \gg a_B$,

$$\varphi_{\text{ind}}(\mathbf{r}) = -\frac{(\boldsymbol{d}\cdot\boldsymbol{r})}{r^3}, \quad \mathbf{E}_{\text{ind}}(\mathbf{r}) = -\frac{\mathbf{d}}{r^3} + \frac{3(\mathbf{d}\cdot\mathbf{r})\mathbf{r}}{r^5}. \tag{2}$$

Due to the small but nonzero energy splitting Δ between $2s$ and $2p$ states (Lamb shift), one needs to apply a small but finite external field, $E_{ext} > \Delta/d$, to create the mixed state (1) and hence to induce the dipole field (2). Importantly, the induced field (2) is much larger than E_{ext}.

One can also look at the problem from another point of view. Consider two hydrogen atoms each in the $n=2$ state. The attractive potential between the atoms has two distinct regimes depending on the distance r between the atoms. The characteristic distance r_Δ is defined by the condition $d^2/r_\Delta^3 \sim \Delta$. If $a_B \ll r \ll r_\Delta$ the potential is

$$V \sim -\frac{d^2}{r^3}. \tag{3}$$

In this regime the electric dipole fields of the two atoms lock to each other. At $r \gg r_\Delta$ the interaction scales as $1/r^6$, this is the usual van der Waals regime that is due to fluctuating dipoles. We will argue below that the dipole distortion of the spin fabric in the 2D *t-J* model shown in Fig. 1 is fully analogous to Eqs. (2) and (3). The power in the 2D case is different, $\frac{1}{r^3} \to \frac{1}{r^2}$. A more important difference is that in the *t-J* model the ground state itself is a parity doublet. The splitting in the doublet is parametrically small at small binding energy, it scales as $\Delta \propto \epsilon^2$, where ϵ is the binding energy.

III. FREE HOLE PROPAGATION IN THE *t-J* MODEL

The 2D *t-J* model was suggested two decades ago to describe the essential low-energy physics of high-T_c cuprates.[7–9] In its extended version, this model includes additional hopping matrix elements t' and t'' to second- and third-nearest Cu neighbors. The Hamiltonian of the *t-t'-t''-J* model on the square Cu lattice has the form:

$$H_{t-J} = -t\sum_{\langle ij\rangle\sigma} c^\dagger_{i\sigma}c_{j\sigma} - t'\sum_{\langle ij'\rangle\sigma} c^\dagger_{i\sigma}c_{j'\sigma} - t''\sum_{\langle ij''\rangle\sigma} c^\dagger_{i\sigma}c_{j''\sigma} + J\sum_{\langle ij\rangle\sigma}\left(\mathbf{S}_i\mathbf{S}_j - \frac{1}{4}N_iN_j\right). \tag{4}$$

Here, $c^\dagger_{i\sigma}$ is the creation operator for an electron with spin $\sigma(\sigma=\uparrow,\downarrow)$ at site i of the square lattice, $\langle ij\rangle$ indicates first-, $\langle ij'\rangle$ second-, and $\langle ij''\rangle$ third-nearest neighbor sites. The spin operator is $\mathbf{S}_i = \frac{1}{2}c^\dagger_{i\alpha}\sigma_{\alpha\beta}c_{i\beta}$, and $N_i = \Sigma_\sigma c^\dagger_{i\sigma}c_{i\sigma}$ is the number density operator. In addition to the Hamiltonian (1) there is the constraint of no double occupancy, which accounts for strong electron correlations.

The values of the parameters of the Hamiltonian (4) for cuprates are known from neutron scattering, Raman spectroscopy, and *ab initio* calculations. For La_2CuO_4 the values are:[10–12]

$$J \approx 140 \text{ meV} \to 1,$$

$$t \approx 450 \text{ meV},$$

$$t' \approx -70 \text{ meV},$$

$$t'' \approx 35 \text{ meV}. \tag{5}$$

Hereafter, we set $J=1$, hence we measure energies in units of J. In the present work we study generic properties of the extended *t-J* model. Therefore we will vary parameters t, t', and t'' in a broad range.

At zero doping (no holes), the *t-J* model is equivalent to the Heisenberg model and describes the Mott insulator La_2CuO_4. The removal of a single electron from this Mott insulator or in other words the injection of a hole, allows the charge carrier to propagate.

The properties of a free single hole in the *t-J* model are very well studied numerically: see Ref. 13 for a review. At values of parameters corresponding to the cuprates the dispersion of the hole dressed by magnetic quantum fluctuations has minima at the 'nodal points' $\mathbf{q}_0 = (\pm\pi/2, \pm\pi/2)$ see Fig. 2. The typical value of the quasiparticle residue at these points is $Z \approx 0.3$. By changing the sign of t' and t'' one can shift the dispersion minima to the "antinodal points" $(\pm\pi, 0)$ and $(\pm\pi, 0)$. This situation corresponds to the electron doped cuprates. We will argue below that the properties of the shallow bound state are most interesting and rich in the regime when the minima of the dispersion are at the nodal points. This is the regime which we consider in the present work. The dispersion of the hole dressed by magnetic quantum fluctuations is quadratic in the vicinity of $\mathbf{q}_0$,

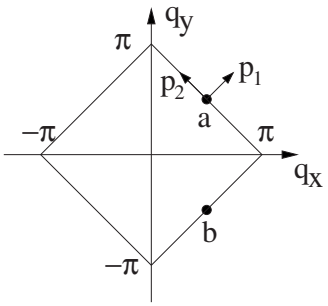

FIG. 2. Magnetic Brillouin Zone with a and b minima of the hole dispersion

$$\epsilon(\mathbf{p}) \approx \frac{1}{2}\beta_1 p_1^2 + \frac{1}{2}\beta_2 p_2^2, \tag{6}$$

where $\mathbf{p}=\mathbf{q}-\mathbf{q}_0$. We set the lattice spacing to unity, 3.81 Å $\rightarrow 1$. In Eq. (6) p_1 is directed along the nodal direction and p_2 is directed along the face of the magnetic Brillouin zone (MBZ), see Fig. 2. At values of the hopping parameters presented in Eq. (5) the inverse masses are,[14] $\beta_1 \approx \beta_2 \approx 2.5$.

It is instructive to consider also the weak coupling limit $t \ll J$ and $t'=t''=0$. In this limit the quasiparticle residue is close to unity, $Z=1-O(t^2/J^2)$, while the dispersion reads[15]

$$\epsilon_{\boldsymbol{q}} = 4t'_{\text{eff}} \cos q_x \cos q_y + 2t''_{\text{eff}}(\cos 2q_x + \cos 2q_y),$$

$$t'_{\text{eff}} \approx 0.25\frac{t^2}{J},$$

$$t''_{\text{eff}} \approx 0.28\frac{t^2}{J},$$

$$\beta_1 = 4t'_{\text{eff}} + 8t''_{\text{eff}} \approx 3.26\frac{t^2}{J},$$

$$\beta_2 = -4t'_{\text{eff}} + 8t''_{\text{eff}} \approx 1.23\frac{t^2}{J}. \tag{7}$$

IV. HOLE BINDING IN THE STRONG COUPLING LIMIT

We include a site-dependant potential attraction to an impurity,

$$H = H_{t-J} + H_U,$$

$$H_U = \sum_{i\sigma} U_i c^\dagger_{i\sigma} c_{i\sigma}. \tag{8}$$

A very important point is that the potential U_i is symmetric around the center of a plaquette, see Fig. 3. Note that the Hamiltonian (8) is written in terms of electrons. Repulsion for electrons $U_i > 0$ corresponds to hole attraction. Concerning the potential we will consider two possibilities. The first possibility is the short-range potential which is nonzero only at four nearest sites, see Fig. 3,

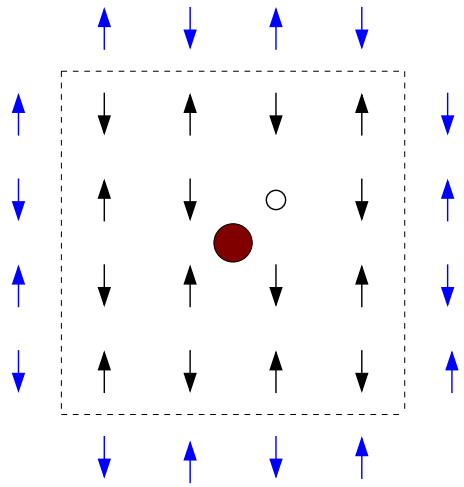

FIG. 3. (Color online). The strong binding limit. Attraction to the potential center (a filled red circle in the center of the plaquette) is so strong that the hole (small empty circle) can hop only within the few sites around the attractive center. In the exact cluster diagonalization we assume that the perimeter spins (blue arrows outside of the dashed square) are static with $\langle S_z \rangle = \pm 0.3$.

$$U_i = U\sum_j \delta_{ij}, \tag{9}$$

where j runs over four nearest sites. The second possibility is the long-range Coulomb interaction

$$U_i = \frac{Q}{\sqrt{r_i^2 + 1}}, \tag{10}$$

where Q is a dimensionless charge which sits at a distance one lattice spacing above the plane.

Let us consider first the local potential (9) in the strong coupling limit, $U \gg t$. The solution of the bound state problem in this limit is qualitatively clear. There are degenerate states with $S_z = \pm\frac{1}{2}$. At each values of S_z there are states of positive and negative parity. Let us consider the lowest bound state in each parity sector. Note that there is only one lowest state in each sector. This is contrary to the common wisdom that the negative parity states are doubly degenerate due to the symmetry of the square lattice (E representation of C_{4v}). The point is that we consider hole binding on the spin background with spontaneously broken SU(2) symmetry. In combination with the impurity potential this breaks the symmetry of the square lattice and, hence, destroys degeneracy of the negative parity states. Binding energies of the lowest bound states are

$$\epsilon_\pm \approx -U \pm \frac{\Delta}{2}. \tag{11}$$

Here the sign $\pm$ denotes the parity of the bound state. We define the binding energy ϵ in the standard way: this is the energy of the bound state taken with respect to the minimum energy of a free hole. So ϵ is always negative. To find the parity splitting Δ in the strong coupling limit we have performed exact diagonalizations of the t-t'-J model on the 16 site cluster shown in Fig. 3. While similar exact diagonaliza-

TABLE I. Exact diagonalization of the 16 site cluster (Fig. 3). The groundstate parity doublet energy splitting and the rms charge radius of the ground state for several values of t and t' and for two values of the confining potential U. According to Eq. (11) $\Delta>0$ corresponds to the negative parity of the ground state and $\Delta<0$ corresponds to the positive parity of the ground state. The bound state results for values of t and t' that correspond to the free hole dispersion minima at the nodal points, $(\pm\pi/2, \pm\pi/2)$, are presented by bold font and underlined.

		$t'=0$		$t'=0.5$		$t'=-0.5$	
t	U	Δ	r_{rms}	Δ	r_{rms}	Δ	r_{rms}
0.25	0	**0.002**	**2.05**	0.562	1.34	−0.558	1.33
0.25	10	**0.024**	**0.71**	0.570	0.72	−0.577	0.72
0.5	0	**0.037**	**1.83**	0.555	1.33	−0.416	1.30
0.5	10	**0.075**	**0.71**	0.567	0.72	−0.547	0.72
1.0	0	**0.096**	**1.60**	0.503	1.32	**−0.079**	**1.09**
1.0	10	**0.172**	**0.72**	0.558	0.73	**−0.283**	**0.73**
2.0	0	**0.062**	**1.26**	0.424	1.25	**0.010**	**1.25**
2.0	10	**0.253**	**0.76**	0.503	0.76	**−0.040**	**0.76**
3.0	0	**0.067**	**1.18**	0.337	1.20	**0.009**	**1.21**
3.0	10	**0.237**	**0.79**	0.431	0.79	**0.004**	**0.80**
4.0	0	**0.066**	**1.17**	0.280	1.18	**0.004**	**1.19**
4.0	10	**0.181**	**0.82**	0.360	0.82	**−0.031**	**0.82**

tions have been performed before,[1–4] the ground-state parity splitting has not been studied systematically, at least these results are not available in literature. The goal of the present section is to study systematically dependence of the ground-state parity splitting on parameters. We have already pointed out that it is qualitatively important to perform the diagonalization on the state with spontaneously broken SU(2) symmetry. Therefore we put the cluster in the environment of static perimeter spins shown in Fig. 3 by blue arrows outside of the dashed square. The magnetization of each static spin has the Heisenberg model value, $\langle S_z\rangle=\pm 0.3$. Values of the splitting Δ within the parity doublet obtained by the 16 site cluster exact diagonalization are presented in Table I. In the same table we present values of the rms charge radius of the lowest bound state. The results are presented for several values of t and t'. The value of t'' in this calculation is zero: the cluster is too small to account for long-range hopping. We have performed the calculation for two values of the confining potential, $U=0$ and $U=10$. In an infinite system the case $U=0$ certainly does not correspond to any binding. However, for the cluster, due to the imposed boundary conditions, the case $U=0$ describes a well localized state of the hole; in this sense it is bound. Our numerical results qualitatively agree with those of previous publications.[1–4] A detailed quantitative comparison is not possible because the previous publications have considered spin symmetric clusters while we impose a spontaneous violation of the SU(2) symmetry via boundary conditions.

The dispersion of a free hole for various values of t and t' is well known from previous work.[13–15] The bound state results in Table I for values of t and t' that correspond to the free hole dispersion minima at the nodal points, $(\pm\pi/2, \pm\pi/2)$, are presented by bold font and underlined. For all other values of t and t' the dispersion minima are at the antinodal points, $(\pm\pi,0)$, $(0,\pm\pi)$, or at the Γ point, $\mathbf{k}=0$. The corresponding bound state results in Table I are shown by standard font. Results presented in Table I lead to the following observations.

(1) Values of the parity splittings for the "nodal cases" (underlined bold font) are very small compared to typical scales in the problem. This conclusion is in agreement with previous observation.[2]

(2) Values of the splittings for other cases (antinodal and "Γ point") are substantially larger.

(3) For each particular "nodal" set of t and t' the splitting Δ for $U=0$ is systematically smaller than that for $U=10$.

The first and second observations indicate that the bound state is close to the parity degeneracy in the case of the nodal minima of the free hole dispersion. This is why in the present work we concentrate on this case. According to the third observation the parity splitting is rapidly decreasing when the radius of the bound state increases. In following section we consider shallow bound states of large radius to confirm these conclusions.

V. HOLE BINDING IN THE WEAK COUPLING LIMIT: THE LEADING APPROXIMATION

Let us look at the binding problem in the weak coupling limit, $U\to 0$ and $\epsilon\to 0$. In this case the shallow bound state

can be built with a hole either from the a or the b valley of the dispersion, see Fig. 2. Hence the bound state has the valley index and the corresponding wave function reads

$$\psi_{\alpha\sigma}(\boldsymbol{r}) = e^{i\boldsymbol{q}_\alpha \cdot \boldsymbol{r}_\sigma}\chi_\alpha(r_\sigma), \tag{12}$$

where $\alpha=a,b$ shows the valley and $\sigma=\uparrow,\downarrow$ shows the magnetic sublattice along which the hole is propagating, r_σ is position on this sublattice. Note that here we have in mind a real propagation. There are also virtual hoppings of the hole to the opposite sublattice. These virtual hoppings lead to formation of the free hole dispersion that was discussed in Sec. III. The z projection of the hole spin is $S_z=-\sigma$. The oscillating exponential dependence $e^{i\boldsymbol{q}_\alpha \cdot \boldsymbol{r}_\sigma}$ in Eq. (12) is due to the momentum $\boldsymbol{q}_\alpha=(\pm\pi/2, \pm\pi/2)$ that corresponds to the valley minimum. The very smooth function $\chi(r)$ exponentially decaying at infinity is due to the hole binding to the potential. In the case of the Coulomb field, Eq. (10), the wave function is[16]

$$\chi = \sqrt{\frac{2}{\pi}}\kappa e^{-\sqrt{2|\epsilon|(r_1^2/\beta_1+r_2^2/\beta_2)}},$$

$$\kappa = \sqrt{\frac{2|\epsilon|}{\sqrt{\beta_1\beta_2}}}. \tag{13}$$

The components r_1 and r_2 in Eq. (13) are projections of $\mathbf{r}$ on directions 1 and 2 corresponding to the particular valley, see Fig. 2. In the case of the local attraction Eq. (9), the wave function is

$$\chi = \frac{\kappa}{\sqrt{\pi}}K_0[\sqrt{2|\epsilon|(r_1^2/\beta_1 + r_2^2/\beta_2)}], \tag{14}$$

where K_0 is the Bessel function of the second kind. Note that for both Eqs. (13) and (14) the root-mean-square radius of the bound state scales as

$$r_{\mathrm{rms}} \propto \frac{1}{\sqrt{|\epsilon|}}. \tag{15}$$

It is easy to see that a change of sign of $\boldsymbol{q}_\alpha$ leads only to a common phase factor in the wave function (12), so this is the same wave function. There are only two distinct possibilities: the a minimum, $\boldsymbol{q}_a=(\pi/2,\pi/2)$ and the b minimum, $\boldsymbol{q}_b=(\pi/2,-\pi/2)$. Thus, there are two degenerate quantum states for each value of S_z.

We put the potential center at the origin of the coordinate system. Then, according to Eq. (12) and Fig. 3 (in this case one has to remove the cluster boundary and extend the figure up to infinity) the $|\uparrow\rangle$ wave functions read

$$\psi_{a\uparrow}(\boldsymbol{r}) = -ie^{i(\pi/2)x_\uparrow + i(\pi/2)y_\uparrow}\chi_a(r),$$

$$\psi_{b\uparrow}(\boldsymbol{r}) = e^{i(\pi/2)x_\uparrow - i(\pi/2)y_\uparrow}\chi_b(r),$$

$$x_\uparrow = \frac{1}{2} + m,$$

$$y_\uparrow = \frac{1}{2} + n, \tag{16}$$

where both $m+n$ and $m-n$ are integer and even. Similarly the $|\downarrow\rangle$ wave functions are

$$\psi_{a\downarrow}(\boldsymbol{r}) = e^{i(\pi/2)x_\downarrow + i(\pi/2)y_\downarrow}\chi_a(r),$$

$$\psi_{b\downarrow}(\boldsymbol{r}) = -ie^{i(\pi/2)x_\downarrow - i(\pi/2)y_\downarrow}\chi_b(r),$$

$$x_\downarrow = \frac{1}{2} + m,$$

$$y_\downarrow = -\frac{1}{2} + n. \tag{17}$$

We put an additional factor $-i$ in $\psi_{a\uparrow}$ and $\psi_{b\downarrow}$ to make these wave functions real. Under the parity operation $x\to -x$ and $y\to -y$, the function $\chi(r)$ does not change. Therefore parities of states (16) and (17) are determined by the phase factors, and the parities are

$$P_{a\uparrow} = e^{i\pi x_\uparrow + i\pi y_\uparrow} = e^{i\pi} = -1,$$

$$P_{b\uparrow} = e^{i\pi x_\uparrow - i\pi y_\uparrow} = e^{i0} = +1,$$

$$P_{a\downarrow} = e^{i\pi x_\downarrow + i\pi y_\downarrow} = e^{i0} = +1,$$

$$P_{b\downarrow} = e^{i\pi x_\downarrow + i\pi y_\downarrow} = e^{i\pi} = -1. \tag{18}$$

Thus, in the leading weak coupling limit approximation, $\epsilon \to 0$, the ground state is a degenerate parity doublet for each value of S_z. This explains why values of the parity splitting presented in Table I by underlined bold font are very small. The next section is addressed at the mechanism that lifts the exact parity degeneracy.

VI. HOLE BINDING IN THE WEAK COUPLING LIMIT: THE SUBLEADING APPROXIMATION

In the present section we demonstrate that in the subleading weak binding approximation, $\epsilon\to 0$, the parity degeneracy of the ground state obtained in the previous section is lifted: the parity splitting scales as $\Delta\propto\epsilon^2$. Because of this scaling the splitting is very small compared to the binding energy, $\Delta \ll \epsilon$.

Signs of the hole wave functions $\psi_{a\uparrow}$ and $\psi_{b\uparrow}$ given by Eq. (16) are shown in Fig. 4. In this case the hole is moving on the "up" sublattice. To avoid misunderstanding we stress that there is only one hole, we do not show spins up in Fig. 4 just to make the figure less busy. The figure clearly demonstrates that the states have opposite parities and different diagonal momenta, $\boldsymbol{q}_a=(\pi/2,\pi/2)$ and $\boldsymbol{q}_b=(\pi/2,-\pi/2)$.

It is clear from Fig. 4 that the difference in energy between states $\psi_{a\uparrow}$ and $\psi_{b\uparrow}$ arises due to diagonal hopping of the hole in the vicinity of the potential, $\Delta\propto t'_{\mathrm{eff}}|\chi(0)|^2$, where t'_{eff} is the effective diagonal hopping that is due to the bare t' and also due to higher orders in t, see, e.g., Eq. (7). Moreover, the splitting cannot be just proportional to $|\chi(0)|^2$; the

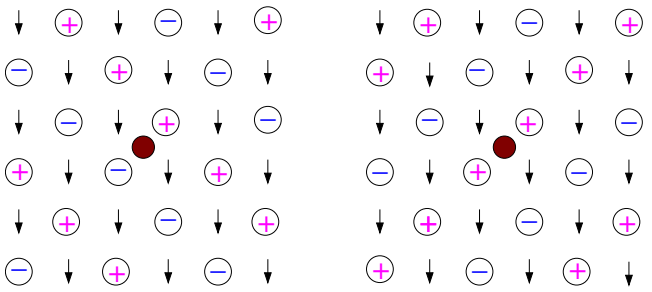

FIG. 4. (Color online). Left: signs of the wave function $\psi_{a\uparrow}$, Right: signs of the wave function $\psi_{b\uparrow}$. The potential center is shown by the filled red circle.

splitting must contain a gradient of χ because there is no a splitting for free hole propagation when χ=const. The first power of the gradient in the energy splitting is forbidden by parity. Thus we come to the following formula for the energy splitting

$$\Delta \propto t'_{\rm eff}|\nabla\chi(0)|^2. \tag{19}$$

The formula contains the second power of gradient, so it is allowed by parity. Having in mind Eqs. (13) and (14) and using Eq. (19) we conclude that

$$\Delta \propto t'_{\rm eff}\kappa^4 \propto t'_{\rm eff}\epsilon^2 \propto \frac{t'_{\rm eff}}{r^4_{\rm rms}}. \tag{20}$$

We stress that this formula follows from general symmetry considerations based on degeneracy of the free hole dispersion at the four nodal points $\boldsymbol{q}=(\pm\pi/2,\pm\pi/2)$. The symmetry arguments certainly do not allow to determine a coefficient in Eq. (20). However, they do allow us to determine the scaling law given by Eq. (20).

It is helpful to support the general considerations presented in the previous paragraph by a numerical calculation. Such a calculation in the regime $t>J$ is hardly possible. However, in the regime $t<J$ the calculation can be performed using results of Ref. 15 summarized in Eq. (7). According to the results the spin quantum fluctuations can be integrated out and the hole propagation on the sublattice up is described by the following effective Hamiltonian

$$H_{\rm eff} = t'_{\rm eff}\sum_{\langle ij'\rangle} h^\dagger_i h_{j'} + t''_{\rm eff}\sum_{\langle ij''\rangle} h^\dagger_i h_{j''}. \tag{21}$$

Here $h^\dagger_i$ is the holon creation operator on the site i; all the sites i, j', and j'' belong to the sublattice up. To be specific we consider here the Coulomb attraction (8) and (10). The attractive interaction written in terms of holon operators reads

$$H_C = -\sum_i U_i h^\dagger_i h_i, \tag{22}$$

where U_i is given by Eq. (10). The Hamiltonian $H_{\rm eff}+H_C$ can be easily diagonalized numerically on a very large cluster. Results of diagonalizations for 30×30 cluster with $t'_{\rm eff}=0.1$, $t''_{\rm eff}=0.25$ and for three values of the dimensionless charge $Q=0.75$, $Q=0.5$, and $Q=0.25$ are shown in Fig. 5. In this figure we show the holon probability distribution for shallow

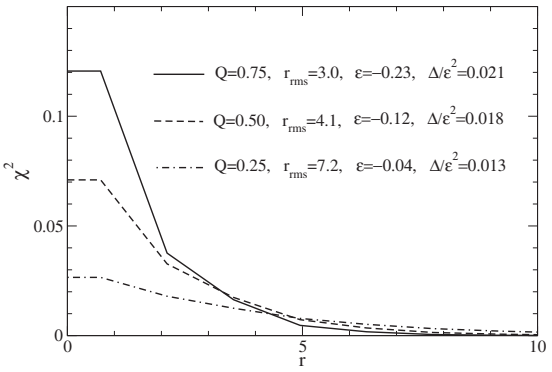

FIG. 5. The shallow Coulomb bound state wave function squared, χ^2, versus radius. Wave functions are shown for three values of the dimensionless charge: $Q=0.75$, $Q=0.5$, and $Q=0.25$. Values of the effective hopping parameters are $t'_{\rm eff}=0.1$ and $t''_{\rm eff}=0.25$. In the legend, for every value of Q we also present the rms radius of the bound state, $r_{\rm rms}$; the binding energy, ϵ; and the ratio of the parity doublet splitting over the binding energy squared, Δ/ϵ^2.

bound states, and in the legends we present values of the rms radius, $r_{\rm rms}$; the binding energy, ϵ; and the ratio Δ/ϵ^2. According to the data in Fig. 5, in the limit $\epsilon\to0$ the parity splitting Δ is decaying even slightly faster than $\propto\epsilon^2$. Most likely the small deviation from the expected ϵ^2 scaling is due to the finite cluster size. We have also checked that the splitting Δ vanishes at $t'_{\rm eff}=0$. Altogether the numerical results presented in Fig. 5 confirm the scaling law given by Eq. (20).

The conclusion of the present section is that the ground state parity splitting is decaying $\Delta\propto\epsilon^2\propto1/r^4_{\rm rms}$ when the binding energy is decreasing, $\epsilon\to0$, $r_{\rm rms}\to\infty$. To estimate the coefficient in this dependence at $t>J$ one can refer to results of exact numerical diagonalizations presented in Table I. It is known experimentally that in very lightly doped $La_{2-x}Sr_xCuO_4$ a hole binding energy to Sr ion is about $\epsilon\approx-10$ meV, the bound state "wave vector" is $\kappa\approx0.4$, and the rms radius of the bound state is $r_{\rm rms}\approx3$, as discussed in Ref. 5 Estimates based on results derived in Secs. IV and VI show that the expected parity splitting of the ground state in this case is a small fraction of 1 meV. Therefore, parity breaking is practically a zero mode of the system.

VII. PARITY BREAKING AND FORMATION OF THE LOCAL SPIN SPIRAL

According to the discussion in previous sections a single hole bound state in the t-J model always has a definite value of the spin projection on the direction of staggered magnetization, $S_z=\pm1/2$, and it always has a definite parity. Dependent on parameters, t, t', etc., the ground state parity can be positive or negative, but it is definite. There is no local spin spiral at this stage. Very close to the ground state there is always a state of opposite parity. Wave functions of these states are given by Eqs. (16) and (17), and parities are given by Eq. (18). Now, following the $2s$-$2p$ hydrogen atom scenario discussed in Sec. II, we can mix the opposite parity states by a weak external perturbation. There are two possibilities: (1) mixing of states with different S_z that belong to

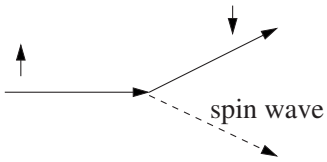

FIG. 6. Hole-spin-wave vertex corresponding to Hamiltonian (24).

the same hole pocket, (2) mixing of states with the same S_z that belong to different hole pockets. In the present section we consider the first possibility that leads to formation of a local spin spiral shown in Fig. 1. The second possibility could lead to formation of a CDW. However, we show in the following section that this possibility is energetically unfavorable.

Thus, let us mix the opposite parity states with different S_z that belong to the same pocket. To do so, we impose a very weak uniform spin twist on the system. At this stage it becomes convenient to use the notation of the nonlinear σ model. In this notation the unit vector $\vec{n}(\boldsymbol{r})$ shows direction of staggered spins. In the antiferromagnetic state the spins are directed along the z axis in the spin space, $\vec{n}=n_z=(0,0,1)$. The uniform spin twist means that the spin direction $\vec{n}$ rotates around a unit vector $\vec{\xi}$ that is orthogonal to the z axis. So locally we can write

$$\delta\vec{n}(\boldsymbol{r}) = (\boldsymbol{Q}\cdot\boldsymbol{r})[\vec{\xi}\times\vec{n}]. \tag{23}$$

Here $\boldsymbol{Q}\ll 1$ is the wave vector of the imposed twist. Let us direct $\boldsymbol{Q}$ along the b nodal direction, see Fig. 2, $\boldsymbol{Q}=Q\boldsymbol{e}_b$, where $\boldsymbol{e}_b$ is the b-nodal unit vector. It is worth noting that generally directions in spin space and directions in the coordinate space are completely independent. The interaction of a hole with the deformation of the spin fabric is of the following form[17]

$$H_{int} = -\sqrt{2}g\vec{\sigma}\times[\vec{n}\times(\boldsymbol{e}\cdot\boldsymbol{\nabla}\vec{n}\,)], \tag{24}$$

where $\boldsymbol{e}$ is a nodal unit vector corresponding to the particular hole, $\vec{\sigma}$ is the Pauli matrix acting on pseudospin of the hole. Note that in the notation of the original t-J model the effective Hamiltonian (24) is just the usual hole-spin-wave vertex shown in Fig. 6. Therefore the coupling constant is $g\approx Zt\approx 1$, where $Z\approx J/t$ is the quasiparticle residue of the hole.

Since $\boldsymbol{Q}=Q\boldsymbol{e}_b$, the interaction (24) does not mix states $\psi_{a\uparrow}$ and $\psi_{a\downarrow}$ however, it does mix states $\psi_{b\uparrow}$ and $\psi_{b\downarrow}$. The corresponding interaction energy is

$$\delta E_{int} = -\sqrt{2}gQ\langle\psi|(\vec{\xi}\cdot\vec{\sigma}\,|\psi\rangle. \tag{25}$$

If the interaction energy is larger than the parity doublet splitting,

$$\sqrt{2}gQ > \Delta, \tag{26}$$

the bound state wave function becomes a mixture of the opposite parity states

$$\psi = \frac{1}{\sqrt{2}}(\psi_{b\uparrow} + e^{i\alpha}\psi_{b\downarrow}), \tag{27}$$

with the phase α determined by the condition $\langle\psi|\vec{\sigma}|\psi\rangle=\vec{\xi}$. Thus, the uniform spin twist Q is completely analogous to a weak uniform electric filed E_{ext} applied to hydrogen atom as has been discussed in Sec. II. The wave function mixing (27) is analogous to the mixing (1). Estimates based on values of Δ obtained in previous sections show that for a bound state with radius $r_{\rm rms}=3$ the twist $Q=0.001-0.002$ is already sufficient to break the parity according to Eqs. (26) and (27). Note that this small value of Q corresponds to a wavelength of about 5000 lattice spacing.

The state (27) possesses a spin-flip dipole moment and hence it creates a long range distortion of the spin fabric as has been discussed in Ref. 5

$$\delta\vec{n}_{\rm ind} = [\vec{\xi}\times\vec{n}]\frac{g}{\sqrt{2}\pi\rho_s}\frac{(\boldsymbol{e}\cdot\boldsymbol{r})}{r^2}[1-e^{-2\kappa r}(1+2\kappa r)]. \tag{28}$$

Here $\rho_s\approx 0.18J$ is the spin stiffness of the Heisenberg model, and κ is the inverse radius of the charge core, see Eq. (13). Equation (28) describes the local spiral depicted in Fig. 1, the local spin spiral is fully analogous to the long-range scalar potential $\varphi_{\rm ind}(\boldsymbol{r})$ generated by an excited hydrogen atom in a tiny external electric field, see Eq. (2).

To derive Eq. (27) and hence to justify the local spin spiral (28) we have introduced a tiny external spin twist that enforces the parity breaking. Alternatively, one can consider an interaction between two holes bound to two impurities separated by a large distance r. Then there is no need for any external twist. Spin spirals induced by different holes lock each other. Hence the spin spiral induced hole-hole interaction is[18]

$$E_S \sim -\frac{g^2}{4\rho_s}\frac{1}{r^2}. \tag{29}$$

This formula is valid at $r<r_\Delta$, while at $r>r_\Delta$ the interaction is $E_S\propto 1/r^4$. Once more, this is absolutely similar to the case of two Hydrogen atoms, see Eq. (3). Estimates based on values of Δ obtained in Secs. IV and VI show that for bound states with radius $r_{\rm rms}=3$ the value of the crossover distance is $r_\Delta\sim 50$. So practically Eq. (29) is always valid. To restore dimension in Eq. (29) one has to recall that $g\approx J\approx 140$ meV, $\rho_s\approx 0.18J$ while dimensionless r is expressed in units of lattice spacing.

VIII. PARITY BREAKING AND POSSIBLE FORMATION OF THE CHARGE DENSITY WAVE

We consider now a possible mixing of the bound states with the same S_z that belong to different hole pockets. Since the spin is not changed there is no deformation of the spin fabric, and a usual electrostatic potential can mix the states. However, the spatial wave functions from different pockets differ by momentum $\boldsymbol{K}=(\pi,0)$ or $\boldsymbol{K}=(0,\pi)$. Therefore, to generate the mixing the electrostatic potential must be modulated at this momentum. So, the mechanism can produce a

CDW with the wave vector $\boldsymbol{K}$. Let ϕ_k is a Fourier component of the external electrostatic potential. The component interacts with the corresponding matrix element of charge density

$$\rho_k = \int \psi^*_{b\uparrow}(\boldsymbol{r}) e^{-i\boldsymbol{k}\cdot\boldsymbol{r}} \psi_{a\uparrow} d^2r$$

$$= \int \chi^2(\boldsymbol{r}) e^{i(\boldsymbol{K}-\boldsymbol{k})\cdot\boldsymbol{r}} d^2r$$

$$= \frac{8\kappa^3}{[4\kappa^2 + (\boldsymbol{K}-\boldsymbol{k})^2]^{3/2}}. \quad (30)$$

We have used here Eqs. (16) and (13). We assume that $\beta_1 = \beta_2$, this allows to evaluate the integral in Eq. (30) analytically. Numerical integration shows that Eq. (30) is approximately valid even with nonequal inverse masses. For example at $\beta_1/\beta_2 = 4$ the deviation from the analytical expression Eq. (30) does not exceed a few percent.

We proceed now directly to the Coulomb interaction between two holes bound to two different impurities separated by large distance r. Since the system is two-dimensional the electrostatic potential created by a charge-density component ρ_k is

$$\phi_k = \frac{2\pi}{k}\rho_k. \quad (31)$$

Therefore the Coulomb interaction energy between two spatially separated bound states reads

$$E_C = -\int \frac{2\pi}{k}\rho_k^2 e^{i\boldsymbol{k}\cdot\boldsymbol{r}} \frac{d^2k}{(2\pi)^2}. \quad (32)$$

Note that the sign is negative because the system always tunes up the mixing phases to reduce energy. Evaluation of Eq. (32) with account of Eq. (30) is straightforward. In the limit $\kappa r \gg 1$ the result reads

$$E_C = -\left(\frac{e^2}{a\epsilon_e}\right)\frac{\kappa^2}{2\pi}(2\kappa r)^2\sqrt{\frac{\pi}{4\kappa r}}e^{-2\kappa r}. \quad (33)$$

Here κ is dimensionless and we put the factor $e^2/(a\epsilon_e) \approx 95$ meV to restore the dimension of energy (e is the elementary charge, $a = 3.81$ Å is the lattice spacing and $\epsilon_e \approx 40$ is the dielectric constant).

Now we can compare the CDW Coulomb interaction (33) with the spin-spiral interaction (29). In the LSCO the "wave vector" of the bound state is $\kappa \approx 0.4$, see Ref. 5. Let us take $r = 4$ that corresponds to the average distance between bound states at the doping level $x \approx 0.06$. With these parameters one finds $E_C \lesssim 1$ meV while $E_S \sim 15$ meV. Thus formation of the CDW is energetically unfavorable compared to formation of the spin spiral.

IX. CONCLUSIONS

We have considered a single hole injected into a two-dimensional Mott insulator on a square lattice with a long range antiferromagnetic order. The system is described by the extended t-J model. An important point is that minima of the hole dispersion are at nodal points $(\pm\pi/2, \pm/\pi/2)$. The hole is bound by an impurity potential. The impurity is located at a center of the lattice plaquette, so the potential itself does not break the local square lattice symmetry.

(1) All bound states have definite parity and they are doubly degenerate with respect to the spin projection on the axis of the staggered magnetization, $S_z = \pm\frac{1}{2}$.

(2) The ground state always has a very close state of opposite parity (parity doublet). For shallow bound states splitting within the parity doublet scales as $\Delta \propto \epsilon^2$, where ϵ is binding energy.

(3) For shallow bound states the parity splitting Δ is extremely small. Therefore an extremely small external twist of the spin fabric breaks parity. The breaking creates a long-range spiral distortion of the spin fabric. The breaking can be also created by another impurity; in this case the local spirals of two impurities lock each other.

(4) The bound state parity breaking in the t-J model is very similar to the parity breaking within the $2s_{1/2}-2p_{1/2}$ parity doublet of the hydrogen atom.

ACKNOWLEDGMENTS

Important discussions with C. Batista and A. Sandvik are acknowledged.

[1] K. J. von Szczepanski, T. M. Rice, and F. C. Zhang, Europhys. Lett. **8**, 797 (1989).
[2] K. M. Rabe and R. N. Bhatt, J. Appl. Phys. **69**, 4508 (1991).
[3] R. J. Gooding, Phys. Rev. Lett. **66**, 2266 (1991).
[4] Yan Chen, T. M. Rice, and F. C. Zhang, Phys. Rev. Lett. **97**, 237004 (2006).
[5] O. P. Sushkov and V. N. Kotov, Phys. Rev. Lett. **94**, 097005 (2005).
[6] O. P. Sushkov, Phys. Rev. B **79**, 174519 (2009).
[7] P. W. Anderson, Science **235**, 1196 (1987).
[8] V. J. Emery, Phys. Rev. Lett. **58**, 2794 (1987).
[9] F. C. Zhang and T. M. Rice, Phys. Rev. B **37**, 3759 (1988).
[10] Y. Tokura, S. Koshihara, T. Arima, H. Takagi, S. Ishibashi, T. Ido, and S. Uchida, Phys. Rev. B **41**, 11657 (1990).
[11] B. Keimer, A. Aharony, A. Auerbach, R. J. Birgeneau, A. Cassanho, Y. Endoh, R. W. Erwin, M. A. Kastner, and G. Shirane, Phys. Rev. B **45**, 7430 (1992).
[12] O. K. Andersen, A. I. Liechtenstein, O. Jepsen, and F. Paulsen, J. Phys. Chem. Solids **56**, 1573 (1995); E. Pavarini, I. Dasgupta, T. Saha-Dasgupta, O. Jepsen, and O. K. Andersen, Phys. Rev. Lett. **87**, 047003 (2001).
[13] E. Dagotto, Rev. Mod. Phys. **66**, 763 (1994).
[14] O. P. Sushkov, G. A. Sawatzky, R. Eder, and H. Eskes, Phys. Rev. B **56**, 11769 (1997).

[15] C. J. Hamer, Zheng Weihong, and J. Oitmaa, Phys. Rev. B **58**, 15508 (1998).
[16] Eq. (13) is exact solution of the Coulomb problem only in the isotropic case, $\beta_1=\beta_2$. In the general anisotropic case Eq. (13) strictly speaking is valid only asymptotically.
[17] B. I. Shraiman and E. D. Siggia, Phys. Rev. Lett. **61**, 467 (1988).
[18] A. Lüscher, A. I. Milstein, and O. P. Sushkov, Phys. Rev. Lett. **98**, 037001 (2007).